Technical University of Denmark

DTU

Ceria based protective coatings for steel interconnects prepared by spray pyrolysis

Szymczewska, Dagmara ; Molin, Sebastian; Chen, Ming; Hendriksen, Peter Vang; Jasinski, Piotr

Link back to DTU Orbit

DTU Library
Technical Information Center of Denmark

11th International Symposium on Systems with Fast Ionic Transport, ISSFIT 11

Ceria based protective coatings for steel interconnects prepared by spray pyrolysis

Dagmara Szymczewska[a], Sebastian Molin[b]*, Ming Chen[b],

Peter Vang Hendriksen[b], Piotr Jasinski[a]

[a]*Faculty of Electronics, Telecommunications and Informatics, Gdansk University of Technology, ul. Narutowicza 11/12, 80-233 Gdansk, Poland*
[b]*Department of Energy Conversion and Storage, Technical University of Denmark, Frederiksborgvej 399, 4000 Roskilde, Denmark*

Abstract

Stainless steels can be used in solid oxide fuel/electrolysis stacks as interconnects. For successful long term operation they require protective coatings, that lower the corrosion rate and block chemical reactions between the interconnect and adjacent layers of the oxygen or the hydrogen electrode. One of the promising coating materials for the hydrogen side is ceria. Using standard sintering techniques, ceria sinters at around 1400°C which even for a very short exposure would destroy the interconnect. Therefore in this paper a low temperature deposition method, i.e. spray pyrolysis, is used to deposit thin (~400 nm), continuous CeO_2 layers on Crofer 22 APU steel substrates. Influence of the deposition parameters on layer quality is elucidated in this work.

1. Introdustion

High temperature solid oxide fuel/electrolysis devices may become a key technology in future efficient energy generation/storage systems [1]. Fuel cells offer high electrical efficiency and also high total efficiency if the heat is

* Corresponding author. Tel.: +45 4677 5296.
  E-mail address: sebmo@dtu.dk

used in combined heat and power units [2]. High temperature electrolysis cells are efficient to convert electrical energy from intermittent sources into chemical energy in form of H_2 and O_2 (or other fuels after adding various upgrading). First commercial high temperature fuel cell systems are already available.

Among the biggest problems with more widespread commercialization of SOFC and SOEC technologies are their degradation during operation. Several degradation phenomena are responsible for the overall degradation: nickel coarsening and loss of percolation, decomposition of electrodes, poisoning by impurities in gasses, chromium poisoning, etc. In consequence ohmic resistance increases. One of the most important degradation mechanisms is connected to high temperature corrosion of metallic interconnects [3,4].

Interconnects of high temperature fuel and electrolysis cells are an important part of the overall fuel cell stack assembly [5,6]. Interconnects separate physically hydrogen and oxygen electrode compartments. They must be electronically conductive in order to pass electrons between neighboring cells. Any rise in their electronic resistivity will add up to the total degradation of the stacks and lower their performance in terms of reducing production capacity per unit cell area.

Interconnects are always exposed to two atmospheres and in both an oxide scale forms. Corrosion rates on both sides for non modified samples are of the same order of magnitude ($k_p \sim 10^{-14}$ g^2 cm^{-4} s^{-1} at 800°C) with a weak tendency to increase with an increase of pO_2 [7]. For the oxygen side, due to possible chromium evaporation and oxygen electrode poisoning, over the years many protective coatings have been developed [4,8]. They have a double beneficial effect of blocking chromium evaporation and also limiting the oxide scale formation effectively lowering corrosion rates by a factor of ~3-10 [4,8,9]. However, as the oxygen side becomes protected against corrosion, the hydrogen side may become the limiting factor for long term operation.

The lifetime of the interconnect (and thus the stack) can be defined in many ways. One of the possibilities is that the formed oxide should not be thicker than 10 µm due to risk of scale spallation and contribution to electrical resistivity. Another way is that the area specific resistance of the interconnect should not exceed a certain threshold (~0.1 Ω cm^{-2}). As the oxide growth kinetics are similar on both sides of the interconnect, it is apparent that some strategies to lower corrosion rates on the hydrogen side are needed.

Moreover, other phenomena than oxide growth might determine the lifetime of the interconnect on the hydrogen side. Several authors have already shown that there is a diffusion of nickel from the contact layer/hydrogen electrode into the steel interconnect [10–12]. Also iron and chromium diffuse to the electrode and might cause its electrochemical deactivation in the long term. Nickel diffusing into ferritic steel can cause its austenitization and sensitization towards carbon containing fuels.

Protective coating for the hydrogen side should reduce corrosion rate at low pO_2 and also mitigate undesired chemical diffusion phenomena. So far, however, studies of coatings for the hydrogen side (especially including corrosion kinetics data) are scarce. Froitzheim et al. [10] studied coatings of CeO_2 and a dual layer of Cu and CeO_2 in hydrogen. Ceria was selected as it is a relatively good n-type electronic conductor (its conductivity increases with the decrease of the pO_2). As presented in [10] its conductivity on the anode side can reach ~0.5 S cm^{-1}. 4 µm thick CeO_2 layer was deposited on Crofer 22 APU by magnetron sputtering. Samples were tested for reaction with Ni by applying a Ni coating on top and exposing for 1000 hours to Ar-$4H_2$-$2H_2O$ atmosphere. On samples without the ceria coating, nickel diffused into steel up to ~75 µm whereas for ceria coated sample neither nickel diffused into steel nor iron and chromium diffused out to nickel. Ceria and doped ceria are widely used materials in high temperature fuel cells [13], ranging from catalytic materials to electrolyte and barrier layers between oxygen electrodes and zirconia electrolytes. Therefore, this material seems well suited for a protective coating on the hydrogen side. Also as a rare earth element, it should have positive effect on reducing corrosion rates [14–16].

In this paper a low temperature (~400°C) spray pyrolysis method is used to deposit thin ceria layers on Crofer 22 APU substrates for the evaluation for their corrosion behavior in humidified hydrogen. Spray pyrolysis was used previously to deposit electrolyte layers and cathodes but was not used for interconnect coatings [17,18]. This work focuses on characterization of different coating thicknesses and coating parameters on the layer quality.

2. Experimental

Coatings of ceria were prepared by spray pyrolysis on Crofer 22 APU 20 x 20 x 0.3 mm^3 substrates. Before the deposition samples were cleaned in ethanol in an ultrasonic bath. The spray pyrolysis setup consists of a spraying

gun placed above a hot plate on which sample is placed. The gun is fed with the spraying solution and the deposition is driven by compressed air. For the coating, the hot plate temperature was held at 400°C. Spraying solutions were prepared by dissolving cerium nitrate in a mixture of tetraethyleneglycol, ethanol and PEG600. Solution was fed to the gun at a rate of 1.5 ml h^{-1}. To obtain different coating thickness (50nm and 100nm), the spraying time was varied between approximately 2.5 and 21hours. In order to prepare thicker coatings (400nm) the deposition procedure was repeated 3 times. The effect of an intermediate annealing of samples at 600°C in-between coating steps was evaluated (sample 400nm_B). Deposition parameters are summarized in Table 1.

Table 1. Description of prepared samples with deposition parameters

Sample name	CeO_2 thickness	Deposition temperature:	Number of depositions:	Deposition time:	Intermediate heating:
50nm	50 nm	400°C	1x	2 h 36 min	No
100nm	100 nm	400°C	1x	7 hours	No
400nm_A	350 nm	400°C	3x	3x 7 hours	No
400nm_B	430 nm	400°C	3x	3x 7 hours	Yes, 600°C

The as-deposited coatings were characterized by x-ray diffractometry (XRD) using a Bruker D8 Advance diffractometer. Grazing incidence x-ray diffractometry (GI-XRD) geometry was used in order to obtain a better signal from the thin films. A grazing angle of 0.3° was used and the scans were performed in the 20°-85° range. Scanning electron microscopy (SEM) was used to evaluate the surface of samples using a Hitachi TM3000 microscope with a Bruker SDD energy dispersive analysis (EDS) detector for chemical analysis. Cross sections were prepared by embedding samples in epoxy and polishing down to 1 µm by using a Struers automated polishing system with diamond suspensions. Cross sections were analyzed by a field emission SEM Zeiss Supra 35.

3. Results and discussion

Surface scanning electron images of samples in the as-prepared state are presented in Figure 1. For samples coated only with one deposition cycle (50nm and 100nm) marks from single droplets are clearly visible. Upon heating the heated surface droplets form a splat that is drying and creating a coating. Most of the visible rings are of ~50 µm in diameter when deposited on the surface. In general in the spray cone wide range of droplet sizes exist with an unknown distribution. Due to the surface tension and edge effects, there is usually more liquid on the edge than in the middle. Therefore, after the drying and decomposition a rim is formed. The concentration of the cations in the solvent is however very low and the rim is only slightly higher than the average. In consequence of prolong deposition time of droplets, the rim effect averages and as a result a uniform coating is formed. It was confirmed that the surface looks uniform without any visible splats in case of the coat thickness of about 300 nm.

Too thick coating obtained during uninterrupted deposition leads to coat cracking. It was evaluated experimentally, that to obtain the coat without any cracking the maximum coat thickness deposited uninterruptedly is around 100 nm. Therefore to coat thicker layers, multiple depositions are required. In this work two methods for obtaining thicker coatings were investigated. In the first one (samples denoted 400nm_A), after a single coating at 400°C the sample was cooled down to room temperature and then heated back to 400°C and coated again. In the second one, after coating at 400°C the sample was cooled to room temperature and then heated in the furnace to 600°C, cooled down and used for another deposition cycle. Intermediate cooling/heating serve to remove mechanical stresses developed in the films during coating. As the layers are formed from the decomposed nitrates, they always contain some organic residues and they are also mostly amorphous after the deposition. The layers are therefore also highly defected and under tension. If the thickness increases above some threshold (depending in each case on the material, temperature, concentration etc.) the coating cracks. As presented in Figure 2 on higher magnification SEM images, some cracks are visible on the sample 400nm_A, which was not treated at higher temperature. No cracks are however observed on the surface for the sample 400nm_B. Therefore the heat treatment seems necessary in order to obtain layers with very high quality.
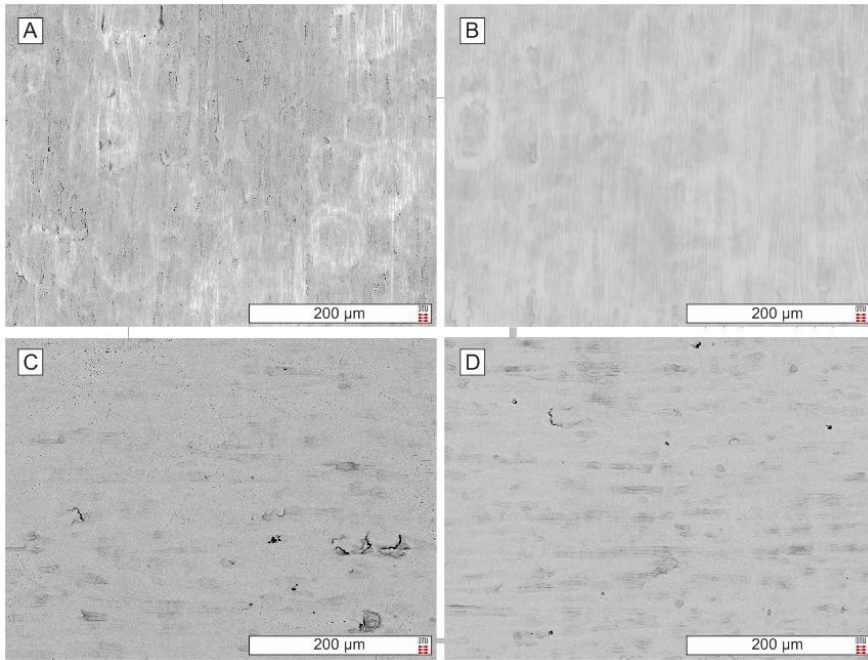
Figure 1. Surface SEM images (magnification 500x) of as prepared coated samples: A - 50nm, B - 100mn, C - 400nm_A and D - 400nm_B.
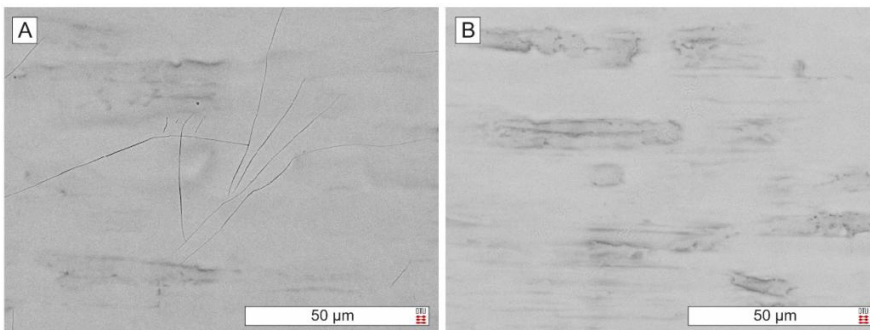

Figure 2. Higher magnification (2000x) SEM of the surface of A – 400nm_A and B – 400nm_B sample.

In order to check the quality of the surface coverage by the coating, the elemental composition of the surface was analyzed by energy dispersive x-ray spectroscopy. This was also used to determine the average amount of Ce deposited on the surface. Figure 3 presents SEM image and elemental mappings of Ce, Fe, Cr and O for all samples. For samples 50nm and 100nm the ceria signal is not uniform and some rings coming from single splats can be observed. These are rich in Ce and poor in Fe. It seems however that whole surface is coated anyway by a thin ceria layer. In case of samples 400nm_A and 400nm_B the cerium signal is more even on the sample. On some places still Fe is more intense but the quality seems satisfactory. In addition to these elements, no other impurities were detected on the surface of the samples.

Table 2 presents the results of the compositional analysis (based on the integrated EDS signal from whole image surface) of the samples surfaces. The amount of Ce detected in the samples is ranging from 3.1 at.% for sample 50nm to ~25 at.% for 400nm samples. Although EDS is not the best method to study chemical compositions of the
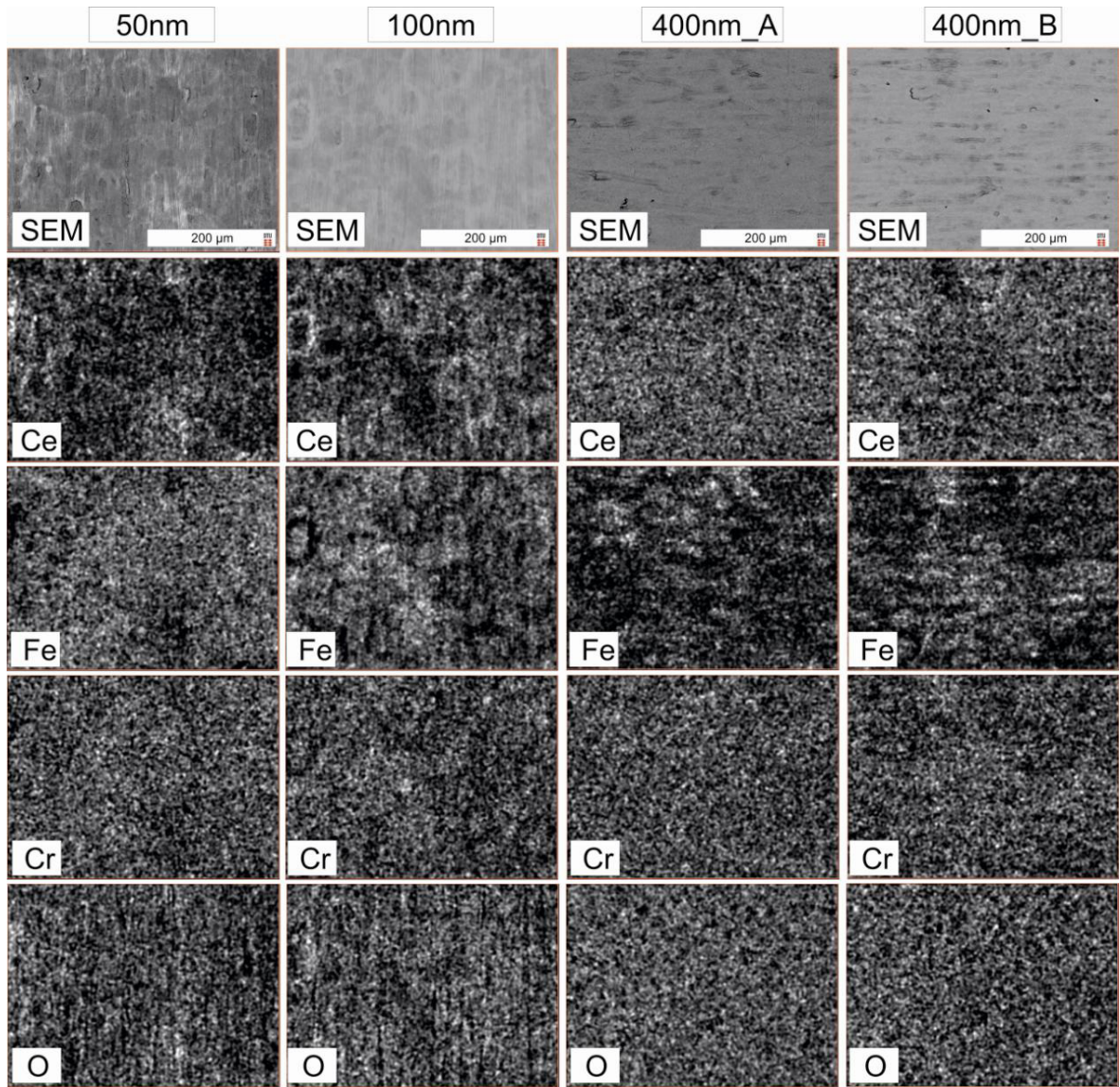
Figure 3. Energy dispersive x-ray spectroscopy elemental analysis of coated samples.

Table 2. Chemical composition of the coated samples as studied by the surface EDS analysis

Sample name	Ce	Fe	Cr	O
	at. %	at. %	at. %	at. %
50nm	3.1	55.1	17.9	23.9
100nm	10.1	33.4	12.5	44.0
400nm_A	27.7	6.6	4.2	61.5
400nm_B	25.7	9.1	6.3	58.8

surfaces due to the relatively large interaction volume of the x-ray beam, it can be used to qualitatively and nondestructively asses the difference between samples. For both samples with 400nm thick layer, the amount of detected Ce is similar. Iron and chromium for uncoated Crofer 22 APU alloy should be approximately around 78 at.% and 21 at.% (plus some minor addition of Mn, Ti and La). For 400nm samples the steel substrate is well screened by the deposited coating.

By evaluating the surface microscopy and elemental analysis it can be concluded that uniform layers with a controlled amount of ceria can be deposited on the surface of steel by means of the spray pyrolysis method.

For phase determination, a grazing incidence x-ray diffractometry was performed on the as-produced coatings. Measured patterns are presented in Figure 4. For samples 50nm and 100nm no signal could be attributed to CeO_2 phase. A peak from the steel substrate is visible at around 46°. For both samples 400nm_A and 400nm_B peaks could be clearly attributed only to the cubic CeO_2 (ICDD card number 34-394) phase. No clear difference between patterns of 400nm_A and 400nm_B are observed, though the low intensity peaks with 222 and 400 indices seem more clearly distinguishable on the heat treated sample. Already after 400°C ceria is crystalline and further exposure to 600°C does not increase the signal strength or narrowness of the peaks. No other phases in addition to CeO_2 (and steel in case of 50nm and 100nm) were detected.
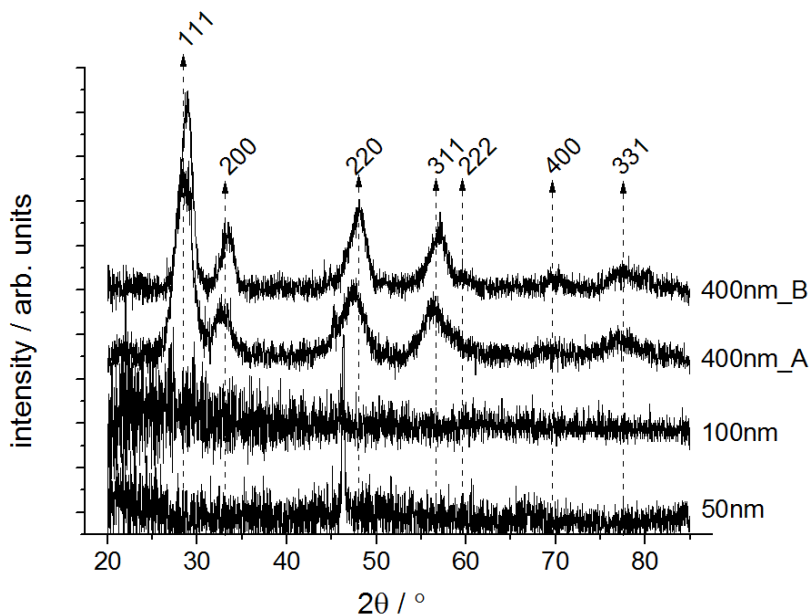

Figure 4. Grazing incidence x-ray diffractometry patterns of samples.

After the surface analysis samples cross sections were analyzed by a high resolution scanning electron microscope. Polished cross sections images of samples are shown in Figure 5. Respective thicknesses of the coatings were measured to be 50 nm (Figure 5 A), 100 nm (Figure 5 B), 350 nm (Figure 5 C) and 430 nm (Figure 5 D).

Taking into account thickness and electrical conductivity of ceria in reducing conditions, we can calculate the theoretical Area Specific Resistance contribution of the introduced layer. Ceria can however have different extrinsic dopants that might change its conductivity thus this consideration should be taken with care. The contribution from the 400 nm thick ceria coatings would be less than 0.1 mΩ cm^2 which is a very small value (~0.1% of the higher limit of the ASR value). Contributions from thinner coatings would be even smaller. Therefore it is not expected that this coatings will have a negative effect on the ASR values for the interconnect even if contact is only established on a small fraction of the surface.

In all cases the surfaces of the Crofer 22 APU substrates seemed to be uniformly covered. The layer was continuous and no cracks were visible. In case of samples 400nm_A and 400nm_B no clear difference in the cross section was visible, thus not directly confirming the cracking as seen in Figure 2. It might be possible that only one

of the 3 deposited layers crack and the coating still seems intact and impermeable in general. Overall the coating quality as analyzed on the cross section images seems very good for further studies.
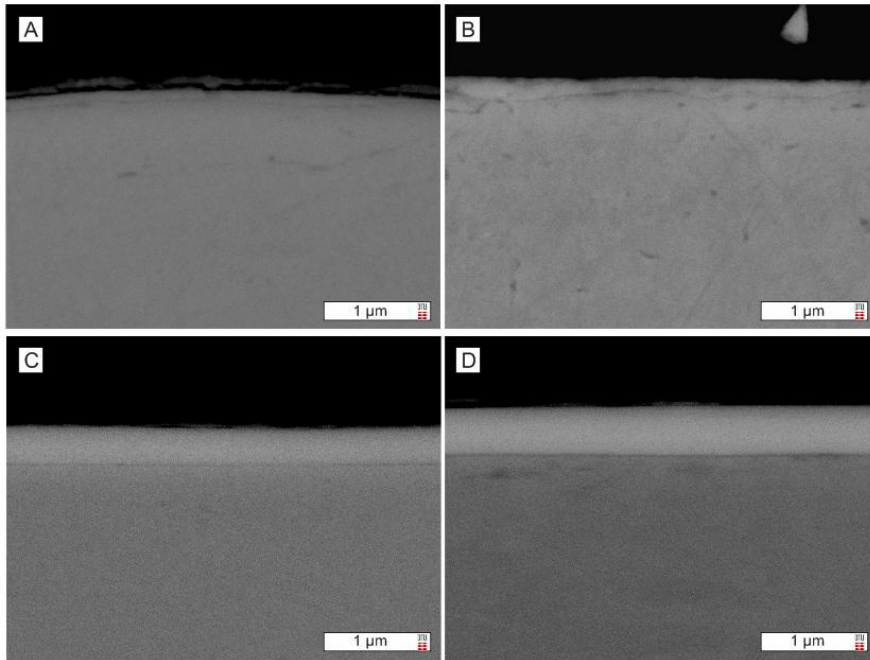

Figure 5. Cross section images of the CeO$_2$ coated Crofer 22 APU substrates. A – 50 nm, B – 100 nm, C – 400nm_A and D – 400nm_B.

4. Summary

In this work the spray pyrolysis deposition method was used to prepare thin ceria layers to be tested as protective coatings for interconnects working in the simulated hydrogen atmosphere. Cross plane conductivity and corrosion properties are currently under investigation and will be reported in the future. Spray pyrolysis, based on the in-situ formation of dense coatings by the use of nitrate solutions allows deposition of uniform layers covering whole surface with good reproducibility. Processing temperature does not exceed 400°C and even at this low temperature dense and crystallized layers can be obtained. Obtaining dense layers of ceramic materials at low temperatures is a critical issue in developing coatings for the hydrogen side, where most of the standard materials require high temperature sintering step, that would normally lead to rapid corrosion of the steel substrate. Therefore ceria layers prepared in this work seem to be promising candidates as protective coatings for the hydrogen side of the interconnects.

Acknowledgements

References

[1]   M.A. Laguna-Bercero, Recent advances in high temperature electrolysis using solid oxide fuel cells: A review, J. Power Sources. 203 (2012) 4–16.
[2]   S.M. Haile, Fuel cell materials and components, Acta Mater. 51 (2003) 5981–6000.
[3]   F. Jeffrey W., Synergism in the design of interconnect alloy–coating combinations solid for oxide fuel cells, Scr. Mater. 65 (2011) 73–77.
[4]   N. Shaigan, W. Qu, D.G. Ivey, W. Chen, A review of recent progress in coatings, surface modifications and alloy developments for solid oxide fuel cell ferritic stainless steel interconnects, J. Power Sources. 195 (2010) 1529–1542.
[5]   P. Piccardo, R. Amendola, S. Fontana, S. Chevalier, G. Caboches, P. Gannon, Interconnect materials for next-generation solid oxide fuel cells, J. Appl. Electrochem. 39 (2009) 545–551.
[6]   W.Z. Zhu, S.C. Deevi, Development of interconnect materials for solid oxide fuel cells, Mater. Sci. Eng. A. 348 (2003) 227–243.
[7]   M. Palcut, L. Mikkelsen, K. Neufeld, M. Chen, R. Knibbe, P.V. Hendriksen, Corrosion stability of ferritic stainless steels for solid oxide electrolyser cell interconnects, Corros. Sci. 52 (2010) 3309–3320.
[8]   S. Molin, M. Chen, P.V. Hendriksen, Oxidation study of coated Crofer 22 APU steel in dry oxygen, J. Power Sources. 251 (2013) 488–495.
[9]   M. Palcut, L. Mikkelsen, K. Neufeld, M. Chen, R. Knibbe, P.V. Hendriksen, Efficient dual layer interconnect coating for high temperature electrochemical devices, Int. J. Hydrogen Energy. 37 (2012) 14501–14510.
[10]   J. Froitzheim, L. Niewolak, M. Brandner, L. Singheiser, W.J. Quadakkers, Anode Side Diffusion Barrier Coating for Solid Oxide Fuel Cells Interconnects, J. Fuel Cell Sci. Technol. 7 (2010) 031020–7.
[11]   J. Malzbender, P. Batfalsky, R. Vaßen, V. Shemet, F. Tietz, Component interactions after long-term operation of an SOFC stack with LSM cathode, J. Power Sources. 201 (2012) 196–203.
[12]   K.A. Nielsen, A.R. Dinesen, L. Korcakova, L. Mikkelsen, P. V Hendriksen, F.W. Poulsen, Testing of Ni-Plated Ferritic Steel Interconnect in SOFC Stacks, Fuel Cells. 6 (2006) 100–106.
[13]   M. Mogensen, N.M. Sammes, G.A. Tompsett, Physical , chemical and electrochemical properties of pure and doped ceria, 129 (2000) 63–94.
[14]   W. Liu, F. Cao, L. Chang, Z. Zhang, J. Zhang, Effect of rare earth element Ce and La on corrosion behavior of AM60 magnesium alloy, Corros. Sci. 51 (2009) 1334–1343.
[15]   G. Bonnet, G. Aguilar, J. Colson, J. Larpin, The effect of rare earths deposited on steel surfaces, by different processes (sol/gel, electrophoresis, OMCVD), on high temperature corrosion behaviour, Corros. Sci. 35 (1993) 893–899.
[16]   D.P. Whittle, J. Stringer, Improvements in High Temperature Oxidation Resistance by Additions of Reactive Elements or Oxide Dispersions, Philos. Trans. R. Soc. London. Ser. A, Math. Phys. Sci. 295 (1980) 309 –329.
[17]   B. Scherrer, J. Martynczuk, H. Galinski, J.G. Grolig, S. Binder, A. Bieberle-Hütter, et al., Microstructures of YSZ and CGO Thin Films Deposited by Spray Pyrolysis: Influence of Processing Parameters on the Porosity, Adv. Funct. Mater. 22 (2012) 3509–3518.
[18]   J. Will, A. Mitterdorfer, C. Kleinlogel, D. Perednis, L.. Gauckler, Fabrication of thin electrolytes for second-generation solid oxide fuel cells, Solid State Ionics. 131 (2000) 79–96.